Physics Letters B 742 (2015) 80–85

Contents lists available at ScienceDirect

Physics Letters B

www.elsevier.com/locate/physletb

Effective interaction of electroweak-interacting dark matter with Higgs boson and its phenomenology

Junji Hisano [a,b], Daiki Kobayashi [a,*], Naoya Mori [a], Eibun Senaha [a]

[a] Department of Physics, Nagoya University, Nagoya 464-8602, Japan
[b] Kavli IPMU (WPI), University of Tokyo, Kashiwa, Chiba 277–8583, Japan

ARTICLE INFO

Article history:
Received 20 October 2014
Received in revised form 24 December 2014
Accepted 11 January 2015
Available online 14 January 2015
Editor: M. Trodden

ABSTRACT

We study phenomenology of electroweak-interacting fermionic dark matter (DM) with a mass of $\mathcal{O}(100)$ GeV. Constructing the effective Lagrangian that describes the interactions between the Higgs boson and the $SU(2)_L$ isospin multiplet fermion, we evaluate the electric dipole moment (EDM) of electron, the signal strength of Higgs boson decay to two photons and the spin-independent elastic-scattering cross section with proton. As representative cases, we consider the $SU(2)_L$ triplet fermions with zero/nonzero hypercharges and $SU(2)_L$ doublet fermion. It is found that the electron EDM gives stringent constraints on those model parameter spaces. In the cases of the triplet fermion with zero hypercharge and the doublet fermion, the Higgs signal strength does not deviate from the standard model prediction by more than a few % once the current DM direct detection constraint is taken into account, even if the CP violation is suppressed. On the contrary, $\mathcal{O}(10$–$20)\%$ deviation may occur in the case of the triplet fermion with nonzero hypercharge. Our representative scenarios may be tested by the future experiments.

1. Introduction

Nature of the dark matter (DM) in the Universe is one of the longstanding problems in both particle physics and cosmology. The DM abundance observed today is [1]

$$\Omega_{\rm CDM}h^2 = 0.1198 \pm 0.0026, \tag{1}$$

where h denotes the reduced Hubble constant. Much attention has been paid to Weakly-Interacting Massive particles (WIMPs) as the candidates for the DM since it is the natural consequence of physics at the TeV scale where the next physics threshold is expected to show up based on the naturalness argument.

Among the various DM scenarios, one of the simplest ones is that the DM particles are coupled to the standard model (SM) particles only through $SU(2)_L \times U(1)_Y$ gauge interactions. (For earlier studies, see, *e.g.*, [2–4].) In those cases, it is known that the DM particle mass would be completely fixed if the thermal relic explains the DM abundance in Eq. (1). For example, the mass of a fermionic DM that belongs to the $SU(2)_L$ doublet (triplet) with hypercharge $Y = 0$ should be about 1 (3) TeV. Those dark matter particles are realized in the supersymmetric (SUSY) standard model as Higgsino (Wino). In the non-thermal relic scenarios, on the other hand, the DM relic abundance could be satisfied as a result of a non-thermal production of the DM from late decay of some heavy particles such as gravitinos in SUSY models. In such a case, the DM particles do not necessarily have the multi-TeV scale mass, and they could be as light as $\mathcal{O}(100)$ GeV. If so, in addition to the standard DM searches, we may find DM signals indirectly in the collider or low energy experiments, even if they are not directly found.

In this Letter, we study the electroweak-interacting fermionic DM particles with the mass of $\mathcal{O}(100)$ GeV, and discuss their phenomenological consequences in a bottom-up approach. The interactions between the $SU(2)_L$ isospin multiplets and the Higgs boson are described by dimension-five operators. Such effective interactions violate CP symmetry generically, and thus CP-violating observables such as the electric dipole moments (EDMs) of electron, neutron and atoms are predicted. In addition, the effective interactions induce the spin-independent (SI) DM-nucleon elastic-scattering cross section and the Higgs boson decay to diphoton. In this paper we evaluate the electron EDM, the SI DM-nucleon cross

* Corresponding author.
E-mail addresses: hisano@eken.phys.nagoya-u.ac.jp (J. Hisano), koba@th.phys.nagoya-u.ac.jp (D. Kobayashi), m-naoya@eken.phys.nagoya-u.ac.jp (N. Mori), senaha@eken.phys.nagoya-u.ac.jp (E. Senaha).

http://dx.doi.org/10.1016/j.physletb.2015.01.012

section and the Higgs signal strength for the Higgs boson decay to diphoton mode, and confront them with current experimental data. Future prospects are also discussed.

2. Models

In this section, we will describe the effective couplings of the fermionic DM particles with the Higgs boson. Now we assume that the DM particle χ_0 is a fermion with the $SU(2)_L \times U(1)_Y$ gauge charges. The effective Higgs couplings depend on whether χ_0 has the $U(1)_Y$ interaction.

First, let us consider the case that χ_0 does not have the $U(1)_Y$ interaction ($Y = 0$). In this case χ_0 is a neutral component of an isospin-n multiplet χ_i ($i = -n, -n+1, \ldots, +n$) with n integer. We assume for simplicity that χ_i are chiral fermions ($\chi_i = P_L \chi_i$). The gauge interactions and the gauge-invariant mass term are

$$\mathcal{L} = \bar{\chi} i \not{D} \chi - \frac{1}{2} M \left(\bar{\chi^c} \chi + \text{h.c.} \right), \tag{2}$$

where $D_\mu = \partial_\mu + ig/\sqrt{2}(T_+ W_\mu^\dagger + T_- W_\mu) + ig_Z (T_3 - Q s_W^2) Z_\mu + ieQ A_\mu$ with $Q = T_3 + Y$. Here, $(T_\pm)_{jk} (\equiv T_1 \pm iT_2) = \sqrt{n(n+1) - k(k \pm 1)} \delta_{j,k\pm1}$, $(T_3)_{jk} = k\delta_{jk}$, and $\bar{\chi^c}\chi = -\sum_{i=-n}^{n} (-1)^{i-1} \chi_i C \chi_{-i}$. The DM particle χ_0 has the Majorana mass term while other particles with non-zero electric charges j ($\neq 0$) have Dirac ones. We take M real positive in the following.

The DM particle does not have renormalizable interactions with the $SU(2)_L$ doublet Higgs boson H, since it is assumed to be a fermion. Now we take the hypercharge for the Higgs boson 1/2. The interactions are given with higher-dimensional ones, which are induced though integration of heavy particles. The dimension-five operators are

$$\mathcal{L}_H = -\frac{1}{2\Lambda} |H|^2 \bar{\chi^c} (1 + i\gamma_5 f) \chi + \text{h.c.} \tag{3}$$

Here, only the isoscalar couplings appear at the dimension five. While bilinears of isospin-n multiplets include an $SU(2)_L$ adjoint representation, it is antisymmetric if n integer. Those effective interactions are induced, for example, by integration of $SU(2)_L$ ($n \pm 1/2$)-multiplet heavy fermions with hypercharge $Y = \pm 1/2$ at the tree level. In the Wino case, the effective interaction with Higgs boson is generated by integration of the Higgsinos. In this paper, we do not adopt such concrete UV models and we take a bottom-up approach as mentioned above.

The effective couplings with the Higgs boson contribute to the masses for χ_i after the Higgs field gets the vacuum expectation value ($H = (0, v)^T$) as

$$M_{\text{phys}}^2 = M_R^2 + M_I^2, \tag{4}$$

where

$$M_R = M + \frac{v^2}{\Lambda}, \qquad M_I = f \frac{v^2}{\Lambda}. \tag{5}$$

The masses for χ_i are degenerate at the tree level. However, it is known that the electroweak corrections make their masses different so that χ_0 is the lightest. The mass difference between χ_j and χ_{j-1}, $\Delta M_{j,j-1}$, is[1]

$$\Delta M_{j,j-1} = \frac{\alpha_2}{4\pi} (2j-1) \left(f(x_W) - c_W^2 f(x_Z) - s_W^2 f(0) \right) M_{\text{phys}}, \tag{6}$$

where

$$f(z) = \int_0^1 dx (2x+2) \log\left(x^2 + (1-x)z \right). \tag{7}$$

Here, $x_W = m_W^2 / M_{\text{phys}}^2$ and $x_Z = m_Z^2 / M_{\text{phys}}^2$, and α_2 is for the $SU(2)_L$ gauge coupling constant, and s_W ($= \sin\theta_W$) and c_W ($= \cos\theta_W$) are for the Weinberg angle θ_W. When 200 GeV $\lesssim M_{\text{phys}} \lesssim$ 3000 GeV, $\Delta M_{j,j-1} \simeq (2j-1) \times$ (167–174) MeV.

Next, we present the case χ_0 has the $U(1)_Y$ interaction. In this case, χ_0 comes from Dirac fermions of an isospin-n multiplet, ψ_i ($i = -n, -n+1, \ldots, +n$). The gauge interactions and the gauge-invariant mass term are

$$\mathcal{L} = \bar{\psi} i \not{D} \psi - M \bar{\psi} \psi, \tag{8}$$

and the effective interactions of ψ and the Higgs boson are given up to dimension five as

$$\mathcal{L}_H = -\frac{1}{\Lambda_1} |H|^2 \, \bar{\psi} (1 + i\gamma_5 f_1) \psi - \frac{1}{\Lambda_2} H^\dagger T_a H \bar{\psi} (1 + i\gamma_5 f_2) T_a \psi. \tag{9}$$

In this case, the isovector couplings are also allowed. The physical masses for ψ_i receive the corrections from the effective interaction after the electroweak symmetry breaking as

$$M_{\text{phys}}^{(i)2} = M_R^{(i)2} + M_I^{(i)2}, \tag{10}$$

where

$$M_R^{(i)} = M + \frac{v^2}{\Lambda_1} - \frac{1}{2} (T_3)_{ii} \frac{v^2}{\Lambda_2}, \tag{11}$$

$$M_I^{(i)} = f_1 \frac{v^2}{\Lambda_1} - \frac{1}{2} (T_3)_{ii} f_2 \frac{v^2}{\Lambda_2}. \tag{12}$$

When the first term in Eq. (9) gives common corrections to the masses, the second term induces mass splitting among the components of multiplet. We take Λ_2 real without loss of generality and assume it positive for simplicity. The components with larger T_3 are lighter if the CP-violating coupling constant f_2 is negligible. Thus, the lightest state is ψ_n, and we have to take $Y = -n$ so that the lightest state is neutral. On the other hand, if the second term in Eq. (9) is negligible, the masses are degenerate up to the radiative corrections. In the case, the mass difference between particles with electric charges Q and $Q-1$, $\Delta M_{Q,Q-1}$, is given as

$$\begin{aligned} \Delta M_{Q,Q-1} = {} & \frac{\alpha_2}{4\pi} (2Q-1) \left(f(x_W) - c_W^2 f(x_Z) - s_W^2 f(0) \right) M_{\text{phys}} \\ & + \frac{\alpha_2}{4\pi} 2Y \left(f(x_Z) - f(x_W) \right) M_{\text{phys}}, \end{aligned} \tag{13}$$

and then $\Delta M_{Q,Q-1} \simeq (2Q-1) \times$ (167–174) MeV $+ Y \times$ (262–357) MeV for 200 GeV $\lesssim M_{\text{phys}} \lesssim$ 3000 GeV. Thus, the neutral fermion is the lightest only when $Y = \pm n$, unless the tree- and loop-level contributions to the mass of the neutral fermion cancel each others accidentally.

Null results of the DM direct detection give a stringent constraint on the vector coupling of the dark matter particles. Thus, the DM particle has to be a Majorana fermion in order to forbid the vector current interaction. Now let us consider the case of $Y = -n$. The neutral component ψ_n with $T_3 = n$ is decomposed into the Majorana fermions (χ_0 and χ_0') as

$$\psi_n = \chi_0 + i\chi_0', \tag{14}$$

and they should not be degenerate in mass, so that the DM direct detection is suppressed. Such mass splitting is generated by the following fermion-number violating interaction,

[1] The mass difference for $n = 1$ is derived in Ref. [5].

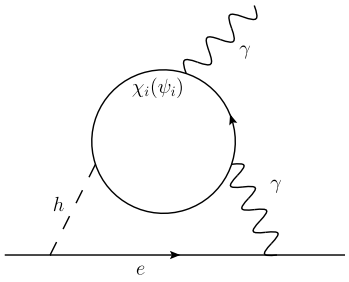

Fig. 1. Barr–Zee diagrams.

$$\mathcal{L}_{HM} = \frac{1}{\Lambda_M^{4n-1}}\left[H^{2n}\bar{\psi}^c\right]\left[H^{2n}\psi\right] + \text{h.c.} \tag{15}$$

where $[\cdots]$ is $SU(2)_L \times U(1)_Y$ invariant. For example, when n is integer, this interaction is generated by integration of heavy fermions of isospin-$(i-1/2)$ multiplets with $Y = -(i-1/2)$ and of isospin-$(i-1)$ multiplets with $Y = -(i-1)$ $(i = 1, \ldots, n)$, which have the Yukawa couplings with the Higgs boson. The isospin singlet fermion with $Y = 0$ has the Majorana mass which is a source of the fermion number violation.

For later use, we collectively denote the Higgs couplings to the fermion fields $(\Psi = \chi_i, \psi_i)$ in the rotated basis as

$$\mathcal{L}_H = -c\bar{\Psi}(g_S + i\gamma_5 g_P)\Psi h, \tag{16}$$

where $c = 1$ $(1/2)$ for Dirac (Majorana) fermions and

$$g_S = \frac{1}{|M_{\text{phys}}|}\left(g'_S M_R + g'_P M_I\right), \tag{17}$$

$$g_P = \frac{1}{|M_{\text{phys}}|}\left(-g'_S M_I + g'_P M_R\right), \tag{18}$$

with $g'_{S,P}$ being the Higgs couplings to the fermion fields in the original basis.

3. Electron EDM, DM direct detection, and Higgs to two gammas

The axial-scalar couplings in Eqs. (3) and (9) are CP violating, so that the EDMs are generated. Now the electron EDM is severely bounded from above from the ACME experiment [6],

$$|d_e| < 8.7 \times 10^{-29}\, e\,\text{cm}, \tag{19}$$

and the bound gives the CP-violating couplings more severe than other EDMs. In this paper we consider constraints on the models using the electron EDM. The bound would be improved to $10^{-(29-30)}\, e\,\text{cm}$ in near future.

The CP-violating Higgs couplings contribute to the electron EDM via the Barr–Zee diagrams at the two-loop level [7]. The Barr–Zee diagrams include the CP-violating anomalous γ–γ–h coupling induced after integrating out χ in Eq. (3) or ψ in Eq. (9), given in Fig. 1. The CP-violating anomalous γ–Z–h coupling is also present, though the contribution to the electron EDM is suppressed due to the accidentally suppressed vector coupling of Z boson with electron, $(1/4 - \sin\theta_W^2) \simeq 0.02$. The CP-violating anomalous γ–W^+–W^- coupling also contributes to the electron EDM. However, the anomalous coupling should be zero at the one-loop level if the components in isospin multiplets are degenerate in mass. Thus, this contribution is also negligible.

By evaluating the diagrams in Fig. 1, we derived the electron EDM in the model in Eq. (3) as

$$\frac{d_e}{e} = \frac{\alpha}{8\pi^3}\frac{m_e M}{M_{\text{phys}}^2}\frac{f}{\Lambda} A_n F(z), \tag{20}$$

where the mass function $F(z)$ $(z = M_{\text{phys}}^2/m_h^2)$ is

$$F(z) = \frac{1}{2}z\int_0^1 dt \frac{1}{t(1-t)-z}\log\frac{t(1-t)}{z}. \tag{21}$$

When $z \gg 1$, $F(z) \simeq \frac{1}{2}\log z + 1$. Since A_n is

$$A_n = \frac{1}{6}n(n+1)(2n+1), \tag{22}$$

the electron EDM is enhanced for large n. In this paper we use $m_h = 125.5$ GeV [8,9].

The electron EDM in the model in Eq. (9) is

$$\frac{d_e}{e} = \sum_i \frac{\alpha}{8\pi^3}\frac{m_e M}{M_{\text{phys}}^{(i)2}}\left(\frac{f_1}{\Lambda_1} - \frac{f_2}{2\Lambda_2}(T_3)_{ii}\right) Q_i^2 F(z_i), \tag{23}$$

where $Q_i = (T_3)_{ii} + Y$. When the masses are degenerate in the multiplets, the electron EDM is reduced as

$$\frac{d_e}{e} = \frac{\alpha}{8\pi^3}\frac{m_e M}{M_{\text{phys}}^{(i)2}}\left(\frac{f_1}{\Lambda_1}A_n^{(1)} - \frac{f_2}{2\Lambda_2}A_n^{(2)}\right) F(z), \tag{24}$$

where

$$A_n^{(1)} = \frac{1}{3}\left(n(n+1) + 3Y^2\right)(2n+1),$$
$$A_n^{(2)} = \frac{2}{3}n(n+1)(2n+1)Y. \tag{25}$$

Then, the contribution from f_2 is more enhanced, especially when $n = \pm Y$.

The Barr–Zee diagram contribution to the electron EDM is suppressed by M_{phys} and Λ. We evaluate the EDM using the effective higher-dimensional interactions in Eq. (3) or ψ in Eq. (9). While those interactions are generated by the some heavy fields, the contributions from the heavy fields to the EDM are suppressed by Λ^2. Thus, we may neglect them as far as $M_{\text{phys}} \ll \Lambda$, and the effective theory description works well for evaluation of the EDM.[2] This is also valid when we consider the Higgs boson decay to diphoton.

In this paper we use the electron EDM bound in order to constrain the parameter spaces. The quark EDMs induced by the Barr–Zee diagrams are related to the electron EDM as $d_q/d_e = (Q_q/Q_e)(m_q/m_e)$. The neutron EDM is given as $d_n \simeq 0.79 d_d - 0.20 d_u$ from the QCD sum rules [11] and the latest neutron EDM bound is $|d_n| < 2.9 \times 10^{-26}\ e\,\text{cm}$ [12]. Thus, the neutron EDM bound is not as stringent as the electron one now.

Next is the Higgs boson decay to two gammas. The signal strength of the Higgs boson decay to two gammas is determined by the low-energy theorem [13–15], and the contribution from the n-multiplet fermions is included as

$$\mu_{\gamma\gamma} = \left|1 + \frac{G_R}{A_{\text{SM}}}\right|^2 + \left|\frac{G_I}{A_{\text{SM}}}\right|^2, \tag{26}$$

where the SM amplitude A_{SM} is -6.49. Here

$$G_R = \sum_i \frac{4\sqrt{2}Q_i^2 v}{3|M_{\text{phys}}^{(i)}|} g_S^{(i)}, \tag{27}$$

$$G_I = \sum_i \frac{2\sqrt{2}Q_i^2 v}{|M_{\text{phys}}^{(i)}|} g_P^{(i)}. \tag{28}$$

[2] The electron EDM is evaluated in UV theories for Wino and Higgsino in Ref. [10].

The measured values of $\mu_{\gamma\gamma}$ at the ATLAS [16] and CMS [17] are respectively given by

$$\mu_{\gamma\gamma} = 1.17 \pm 0.27 \text{ (ATLAS)}, \qquad \mu_{\gamma\gamma} = 1.14^{+0.26}_{-0.23} \text{ (CMS)}. \quad (29)$$

Last, we consider the DM direct detection by elastic scattering with nucleon. It is induced by the DM particle coupling with the Higgs boson. The SI cross section of the DM particle χ^0 with proton is at the leading order,

$$\sigma^p_{\rm SI} = \frac{2}{\pi}\frac{m_p^4 g_S^2}{m_h^4 v^2}\left(\frac{1}{9}f_{TG} + \frac{1}{2}\sum_{q=u,d,s} f_{Tq}\right)^2. \quad (30)$$

(See Refs. [18,19].) Here, m_p is the proton mass, and f_{TG} and f_{Tq} are the nucleon mass fractions of gluon and quarks, respectively. In this paper we use $f_{Tu} = 0.023$, $f_{Td} = 0.032$, $f_{Ts} = 0.020$, $f_{TG} = 1 - \sum_{q=u,d,s} f_{Tq} = 0.925$ [20]. Even if the DM particle has only the electroweak interaction, the SI cross section with proton of the DM particle is induced at the loop level. The contribution is evaluated in Ref. [20]. Since such contributions may be relevant in the large Λ region where Eq. (30) is suppressed, we take them into account in our numerical calculation. Recently, LUX experiment [21] put a new constraint on $\sigma^p_{\rm SI}$. For example, $\sigma^p_{\rm SI} \lesssim 10^{-45}$ cm^2 for the DM with a mass of 100 GeV.

Before going into the numerical analysis, the experimental constraints on $M_{\rm phys}$ are discussed. First, we consider the bounds coming from the Large Hadron Collider (LHC). In the case of $\Delta M_{Q,Q-1} \lesssim 1$ GeV, the dominant decay mode of χ_Q is $\chi_Q \to \chi_{Q-1}\pi^+$. In the Wino case, which is the typical lifetime of $\chi^\pm$ is $\mathcal{O}(0.1)$ ns. Such a metastable charged particle may be probed by looking at the disappearing charged track at the LHC. Using 20.3 fb^{-1} data collected at $\sqrt{s} = 8$ TeV running, the ATLAS collaboration places a lower bound on $M_{\rm phys}$ [22]

$$M_{\rm phys} > 270 \text{ GeV}, \quad (31)$$

at 95% C.L. For larger n, however, the lifetime of χ is so short that we do not obtain a useful constraint by this searches.

When the mass splitting is larger than $\sim$1 GeV, the constraints on $M_{\rm phys}$ from the LHC experiments are weaker. The searches for direct production of charginos and neutralinos in final states with two or three leptons and missing transverse energy are conducted at the LHC. Depending on the lightest neutralino mass (denoted as $m_{\tilde{\chi}^0}$), the limit is placed on the masses of the chargino and the second lightest neutralino which are assumed to be degenerate. For example, the chargino has to be heavier than 415 GeV if $m_{\tilde{\chi}^0} = 0$ while no significant bound is obtained if $m_{\tilde{\chi}^0} \gtrsim 160$ GeV [23,24].

The other constraints may come from indirect DM searches. The comprehensive studies on the indirect detection of the Wino DM are conducted in Ref. [25]. The Wino mass is bounded as

$$320 \text{ GeV} \lesssim M_{\rm phys} \lesssim 2.25 \text{ TeV},$$
$$2.43 \text{ TeV} \lesssim M_{\rm phys} \lesssim 2.9 \text{ TeV}, \quad (32)$$

which are set by gamma-ray observations of classical dwarf spheroidal galaxies and the DM relic abundance constraint. For larger n, the constraints would become more severe if the DM dominates the observed DM abundance in Eq. (1), since the annihilation cross sections of the DM grow as $\mathcal{O}(n^4)$ [3,4]. In this paper, we consider the cases of $n = 1$ and $n = 1/2$, and the other cases are discussed qualitatively.

4. Results

Now, we show our numerical results. First, we consider a case in which $Y = 0$ and $n = 1$ (isospin triplet). In Fig. 2, $|d_e|$, $\sigma^p_{\rm SI}$ and $\mu_{\gamma\gamma}$ are plotted in the (Λ, f) plane. We take $M_{\rm phys} = 400$ GeV as an example. In this case, 370 GeV $\lesssim M \lesssim$ 400 GeV. The black lines, from top to bottom, represent $|d_e^{\rm EXP}| = 8.7 \times 10^{-29}$ e cm, 10^{-29} e cm, 10^{-30} e cm and 10^{-31} e cm, respectively. As shown, Λ has to be greater than around 2(20) TeV for $f = 0.1(1.0)$ to satisfy the current limit. When $M_{\rm phys}$ is heaver, $|d_e|$ is scaled as $1/M_{\rm phys}$.

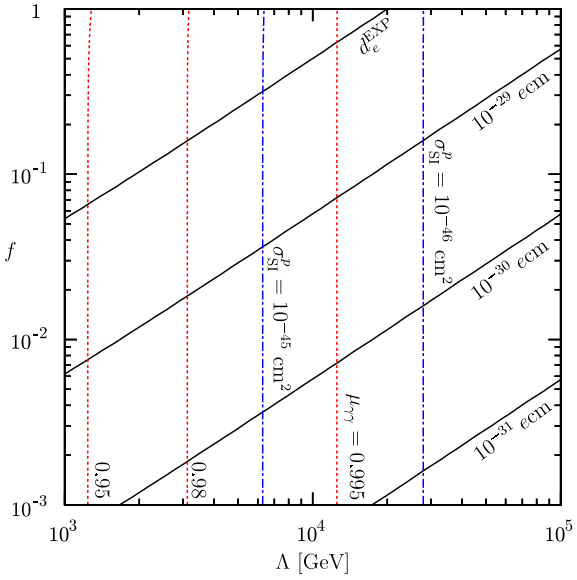

Fig. 2. $|d_e|$ (straight lines in black), $\sigma^p_{\rm SI}$ (dotted-dashed lines in blue) and $\mu_{\gamma\gamma}$ (dotted lines in red) in the case of $Y = 0$ and $n = 1$ (triplet). We set $M_{\rm phys} = 400$ GeV. (For interpretation of the colors in this figure, the reader is referred to the web version of this article.)

The dotted–dashed vertical lines in blue denote $\sigma^p_{\rm SI} = 10^{-45}$ cm^2 and $\sigma^p_{\rm SI} = 10^{-46}$ cm^2 from left to right. It is insensitive to the CP-violating coupling f and also $M_{\rm phys}$. It is found that Eq. (30) becomes smaller than the loop contributions ($\simeq 1.4 \times 10^{-47}$ cm^2) [19,20] for $\Lambda \gtrsim 47$ TeV, and reach around 3.0×10^{-48} cm^2 at $\Lambda = 100$ TeV.

The dotted lines in red represent $\mu_{\gamma\gamma} = 0.95, 0.98$ and 0.995 from left to right. The numerical impact of the fermions with $|Q| = 1$ on $\mu_{\gamma\gamma}$ is less than 2% for $\Lambda \gtrsim 3$ TeV. As seen in Eq. (26), the dominant new physics contribution comes from the CP-conserving part. The deviation of $\mu_{\gamma\gamma}$ from one is scaled as $1/(\Lambda M_{\rm phys})$, and it is less sensitive to f.

Next, we illustrate a case in which $n = 1 = -Y$. Our finding is shown in Fig. 3. For simplicity, we take $f_1 = f_2 \equiv f$, $\Lambda_1 = \Lambda_2 \equiv \Lambda$ and $M = 400$ GeV. Similar to the previous case, we display $|d_e|$, $\sigma^p_{\rm SI}$ and $\mu_{\gamma\gamma}$ in the (Λ, f) plane. The color scheme is the same as in Fig. 2. The fermion masses with $|Q| = 0, 1, 2$ are varied in the following ranges: 400 GeV $\lesssim M^{(1)}_{\rm phys} \lesssim$ 415 GeV, 400 GeV $\lesssim M^{(0)}_{\rm phys} \lesssim$ 431 GeV and 400 GeV $\lesssim M^{(-1)}_{\rm phys} \lesssim$ 448 GeV, respectively. Since there are the fermions with $|Q| = 2$ in this case, the phenomenological consequences are quite different from the previous case. As for the electron EDM constraint, the region where $|d_e/d_e^{\rm EXP}| \leq 1$ is satisfied gets significantly smaller. For instance, Λ must be greater than around 15 TeV for $f = 0.1$, and $f = 1$ is not allowed even if $\Lambda = 100$ TeV.

We observe that $\sigma^p_{\rm SI}$ is reduced to some extent compared to the previous case. In the large Λ region, $\sigma^p_{\rm SI}$ may be as small as $\mathcal{O}(10^{-48})$ cm^2. As shown in Ref. [20], the loop contributions in $\sigma^p_{\rm SI}$ get reduced as Y increases.

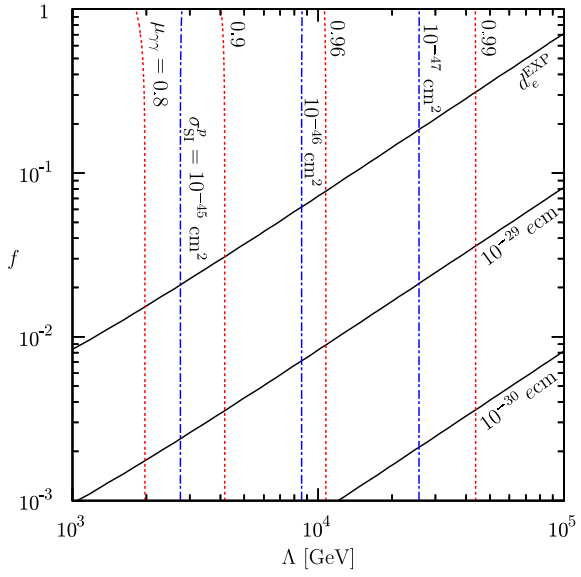

Fig. 3. $|d_e|$, $\sigma_{\rm SI}^p$ and $\mu_{\gamma\gamma}$ in the case of $n = 1 = -Y$ (triplet). We set $f_1 = f_2 \equiv f$, $\Lambda_1 = \Lambda_2 \equiv \Lambda$ and $M = 400$ GeV.

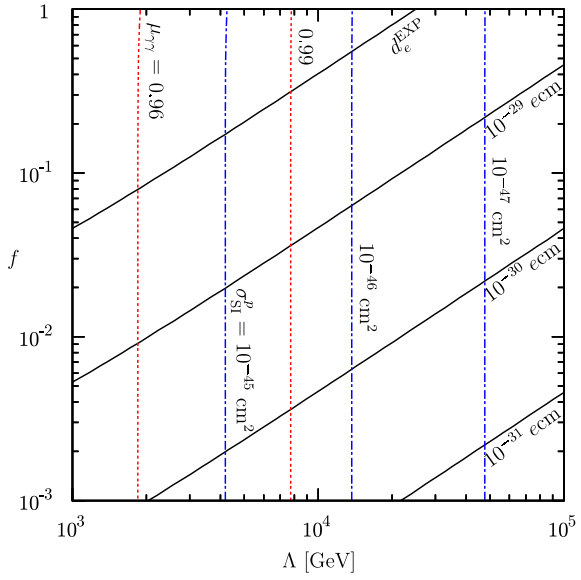

Fig. 4. $|d_e|$, $\sigma_{\rm SI}^p$ and $\mu_{\gamma\gamma}$ in the case of $n = 1/2 = -Y$ (doublet). We set $f_1 = f_2 \equiv f$, $\Lambda_1 = \Lambda_2 \equiv \Lambda$ and $M = 400$ GeV.

It is also found that $\mu_{\gamma\gamma}$ may be significantly reduced. For example, $\mu_{\gamma\gamma}$ may be as small as 0.8 at $\Lambda \simeq 2$ TeV, which is mainly due to the contribution of the fermions with $|Q| = 2$.

In this example, we simply assume $f_1 = f_2$ and $\Lambda_1 = \Lambda_2$. However, we could treat them separately. In such a case, we may have sizable cancellations in d_e by choosing the input parameters judiciously as inferred from Eq. (23), leading to more relaxed bounds.

The results in the case of $n = 1/2 = -Y$ (doublet) are shown in Fig. 4. The input parameters are the same as in Fig. 3. The masses of the fermions with $|Q| = 0, 1$ are varied in the ranges: 400 GeV $\lesssim M_{\rm phys}^{(1/2)} \lesssim$ 423 GeV, 400 GeV $\lesssim M_{\rm phys}^{(-1/2)} \lesssim$ 440 GeV, respectively. Although the particle content is similar to the case of $Y = 0$ and $n = 1$, the electron EDM and $\mu_{\gamma\gamma}$ are somewhat enhanced due to the presence of the second term in Eq. (9). On the other hand, $\sigma_{\rm SI}^p$ gets smaller because of $Y \neq 0$ contributions at the loop level as mentioned above.

We considered the cases of $(n, Y) = (1, 0),\ (1, -1),\ (1/2, -1/2)$. When n is increased, fermions with larger electric charges are introduced. When Y is zero, the electron EDM and deviation of $\mu_{\gamma\gamma}$ from one are scaled by $A_n = n(n+1)(2n+1)/6$. When Y is nonzero, fermions with larger electric charges than in the cases of $Y = 0$ contribute to them so that the larger effects are expected. Furthermore, when the isovector couplings are sizable, the contributions to d_e and $\mu_{\gamma\gamma}$ dominate over those from the isoscalar couplings. On the other hand, $\sigma_{\rm SI}^p$ is insensitive to n when $Y = 0$. If $Y \neq 0$, $\sigma_{\rm SI}^p$ depends on n and Y via the isovector coupling f_2.

Here, we briefly discuss the thermal DM scenario. The results of $(n, Y) = (1, 0),\ (1/2, -1/2)$ are presented in Fig. 5. We do not consider the $(n, Y) = (1, -1)$ case since the correct DM mass in light of the Sommerfeld effect is unknown. Notice that Λ is taken from 10^4 GeV to justify our analysis based on the effective Lagrangians (3) and (9). Since the mass scale of each multiplet is 2900 GeV and 1000 GeV, the deviation of $\mu_{\gamma\gamma}$ from the SM value is less than 1% so that the contour is not shown here. Likewise, the current electron EDM bound is not strong enough to probe this parameter space except the tiny portion in the case of $(n, Y) = (1/2, -1/2)$. As for the DM direct detection in the $(n, Y) = (1, 0)$ case, $\sigma_{\rm SI}^p$ mildly decreases as Λ increases and reach 1.5×10^{-47} cm^2 at $\Lambda = 10^6$ GeV. In the $(n, Y) = (1/2, -1/2)$ case, on the other hand, $\sigma_{\rm SI}^p$ is more suppressed due to the $Y \neq 0$ contributions in the loop corrections as mentioned above.

Finally, we remark some future prospects. The electron EDM is expected to be improved up to $\sim 10^{-30}$ e cm level [26–28]. For the DM direct detection, $\sigma_{\rm SI}^p$ would be improved by more than one order of magnitude by the XENON1T experiment [29], and further improvement is projected by the LZ experiment [30]. The future collider experiments such as the high-luminosity LHC (HL-LHC) [31,32] and International Linear Collider (ILC) [33] may improve the sensitivity of $\mu_{\gamma\gamma}$ up to $\mathcal{O}(5)$%. Combining all data, especially the former two, we may test almost entire region in the nonthermal DM scenario.

5. Conclusion

We have studied phenomenology of electroweak-interacting fermionic dark matter with a mass of $\mathcal{O}(100)$ GeV. Constructing the effective Lagrangian that describes the interactions between the Higgs boson and the SU(2)$_L$ isospin multiplet fermion, we evaluate the electric dipole moment of electron, the signal strength of Higgs boson decay to two photons and the DM direct detection.

As a benchmark point, 400 GeV for SU(2)$_L$ isospin multiplet fermion mass is taken throughout this analysis. In particular, we investigated the three representative cases: (1) triplet fermion with $Y = 0$, (2) triplet fermion with $Y \neq 0$ and (3) doublet fermion with $Y \neq 0$. It is found that the LUX direct detection bound ($\sigma_{\rm SI}^p \sim 10^{-45}$ cm^2) is probing $\Lambda \simeq$ multi-TeV region, and the case (1) suffers from it the most among the three. If the CP-violating Higgs-fermion coupling is unity, the current electron EDM limit pushes the cutoff Λ up to around 20 TeV in the cases (1) and (3) while above 100 TeV in the case (2). In light of the current DM direct detection constraint, the signal strength of the Higgs boson decay to two photons deviates from the SM value by more than a few % in the cases (1) and (3). In the case (2), on the other hand, about 20% deviation of Higgs signal strength is still allowed even though it is out of 1σ range of the current data. Our analysis shows that the unconstrained areas in the all cases would be tested by the future improvements of d_e and $\sigma_{\rm SI}^p$. The HL-LHC and ILC are also important to probe the region of $\Lambda \lesssim 10$ TeV in the case (2).

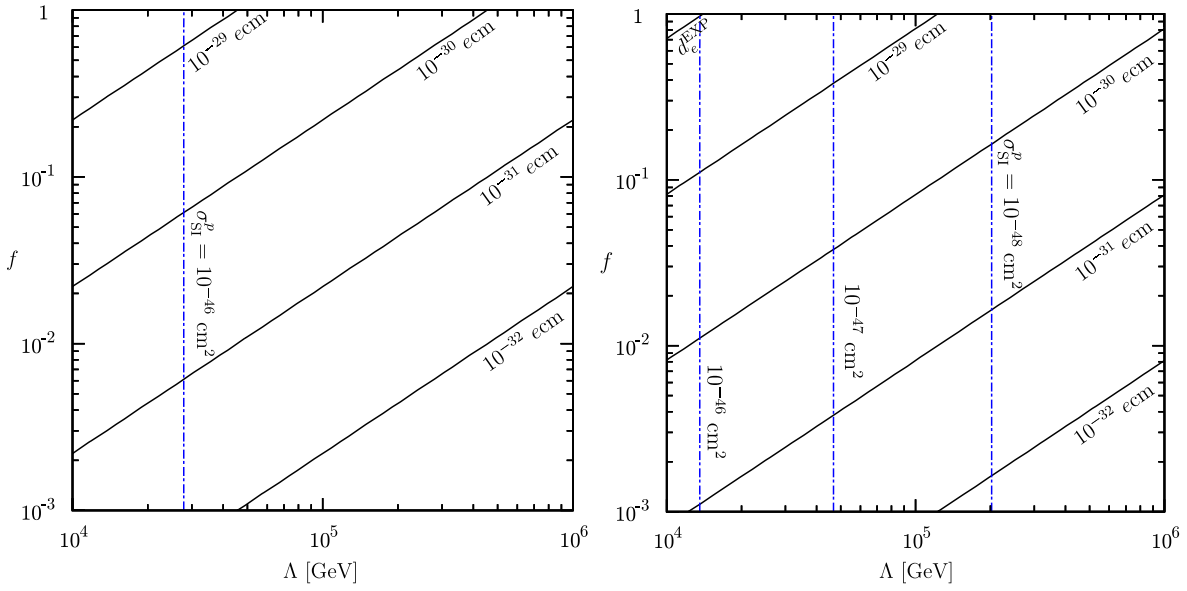

Fig. 5. $|d_e|$ and $\sigma_{\rm SI}^{p}$ in the thermal DM scenario. (Left) $Y = 0$ and $n = 1$, $M_{\rm phys} = 2900$ GeV; (right) $n = 1/2 = -Y$, $M = 1000$ GeV.

Acknowledgements

The work of J.H. is supported by Grant-in-Aid for Scientific research from the Ministry of Education, Science, Sports, and Culture (MEXT), Japan, No. 24340047 and No. 23104011, and also by World Premier International Research Center Initiative (WPI Initiative), MEXT, Japan. The work of D.K. is supported by Grant-in-Aid for Japan Society for the Promotion of Science (JSPS) Fellows (No. 26004521).

References

[1] K.A. Olive, et al., Particle Data Group, Chin. Phys. C 38 (2014) 090001.
[2] J. Hisano, S. Matsumoto, M.M. Nojiri, Phys. Rev. D 67 (2003) 075014;
J. Hisano, S. Matsumoto, M.M. Nojiri, Phys. Rev. Lett. 92 (2004) 031303;
J. Hisano, S. Matsumoto, M.M. Nojiri, O. Saito, Phys. Rev. D 71 (2005) 015007;
J. Hisano, S. Matsumoto, M.M. Nojiri, O. Saito, Phys. Rev. D 71 (2005) 063528;
J. Hisano, S. Matsumoto, O. Saito, M. Senami, Phys. Rev. D 73 (2006) 055004;
J. Hisano, S. Matsumoto, M. Nagai, O. Saito, M. Senami, Phys. Lett. B 646 (2007) 34.
[3] M. Cirelli, N. Fornengo, A. Strumia, Nucl. Phys. B 753 (2006) 178, arXiv:hep-ph/0512090.
[4] M. Cirelli, A. Strumia, M. Tamburini, Nucl. Phys. B 787 (2007) 152, arXiv:0706.4071 [hep-ph].
[5] H.-C. Cheng, B.A. Dobrescu, K.T. Matchev, Nucl. Phys. B 543 (1999) 47, arXiv:hep-ph/9811316.
[6] V.A. Dzuba, V.V. Flambaum, C. Harabati, Phys. Rev. A 84 (2011) 052108.
[7] S.M. Barr, A. Zee, Phys. Rev. Lett. 65 (1990) 21;
S.M. Barr, A. Zee, Phys. Rev. Lett. 65 (1990) 2920 (Erratum).
[8] G. Aad, et al., ATLAS Collaboration, Phys. Rev. D 90 (2014) 052004, arXiv:1406.3827 [hep-ex].
[9] CMS Collaboration [CMS Collaboration], and studies of the compatibility of its couplings with the standard model, CMS-PAS-HIG-14-009.
[10] G.F. Giudice, A. Romanino, Phys. Lett. B 634 (2006) 307, arXiv:hep-ph/0510197.
[11] J. Hisano, J.Y. Lee, N. Nagata, Y. Shimizu, Phys. Rev. D 85 (2012) 114044, arXiv:1204.2653 [hep-ph];
K. Fuyuto, J. Hisano, N. Nagata, K. Tsumura, J. High Energy Phys. 1312 (2013) 010, arXiv:1308.6493 [hep-ph].
[12] C.A. Baker, D.D. Doyle, P. Geltenbort, K. Green, M.G.D. van der Grinten, P.G. Harris, P. Iaydjiev, S.N. Ivanov, et al., Phys. Rev. Lett. 97 (2006) 131801, arXiv:hep-ex/0602020.
[13] M.B. Voloshin, Phys. Rev. D 86 (2012) 093016, arXiv:1208.4303 [hep-ph].
[14] D. McKeen, M. Pospelov, A. Ritz, Phys. Rev. D 86 (2012) 113004, arXiv:1208.4597 [hep-ph].
[15] J. Fan, M. Reece, J. High Energy Phys. 1306 (2013) 004, arXiv:1301.2597.
[16] G. Aad, et al., ATLAS Collaboration, arXiv:1408.7084 [hep-ex].
[17] V. Khachatryan, et al., CMS Collaboration, arXiv:1407.0558 [hep-ex].
[18] G. Jungman, M. Kamionkowski, K. Griest, Phys. Rep. 267 (1996) 195, arXiv:hep-ph/9506380.
[19] J. Hisano, K. Ishiwata, N. Nagata, Phys. Lett. B 690 (2010) 311, arXiv:1004.4090 [hep-ph];
J. Hisano, K. Ishiwata, N. Nagata, Phys. Rev. D 82 (2010) 115007, arXiv:1007.2601 [hep-ph].
[20] J. Hisano, K. Ishiwata, N. Nagata, T. Takesako, J. High Energy Phys. 1107 (2011) 005, arXiv:1104.0228 [hep-ph].
[21] D.S. Akerib, et al., LUX Collaboration, Phys. Rev. Lett. 112 (2014) 091303, arXiv:1310.8214 [astro-ph.CO].
[22] G. Aad, et al., ATLAS Collaboration, Phys. Rev. D 88 (11) (2013) 112006, arXiv:1310.3675 [hep-ex].
[23] G. Aad, et al., ATLAS Collaboration, J. High Energy Phys. 1404 (2014) 169, arXiv:1402.7029 [hep-ex].
[24] G. Aad, et al., ATLAS Collaboration, J. High Energy Phys. 1405 (2014) 071, arXiv:1403.5294 [hep-ex].
[25] B. Bhattacherjee, M. Ibe, K. Ichikawa, S. Matsumoto, K. Nishiyama, arXiv:1405.4914 [hep-ph].
[26] Y. Sakemi, K. Harada, T. Hayamizu, M. Itoh, H. Kawamura, S. Liu, H.S. Nataraj, A. Oikawa, et al., J. Phys. Conf. Ser. 302 (2011) 012051.
[27] D.M. Kara, I.J. Smallman, J.J. Hudson, B.E. Sauer, M.R. Tarbutt, E.A. Hinds, New J. Phys. 14 (2012) 103051, arXiv:1208.4507 [physics.atom-ph].
[28] D. Kawall, J. Phys. Conf. Ser. 295 (2011) 012031.
[29] E. Aprile, XENON1T Collaboration, Springer Proc. Phys. 148 (2013) 93, arXiv:1206.6288 [astro-ph.IM].
[30] P. Cushman, C. Galbiati, D.N. McKinsey, H. Robertson, T.M.P. Tait, D. Bauer, A. Borgland, B. Cabrera, et al., arXiv:1310.8327 [hep-ex].
[31] ATLAS Collaboration, arXiv:1307.7292 [hep-ex].
[32] CMS Collaboration, arXiv:1307.7135.
[33] H. Baer, T. Barklow, K. Fujii, Y. Gao, A. Hoang, S. Kanemura, J. List, H.E. Logan, et al., arXiv:1306.6352 [hep-ph].